JACS
JOURNAL OF THE AMERICAN CHEMICAL SOCIETY
Article
pubs.acs.org/JACS

Perpetually Self-Propelling Chiral Single Crystals

Manas K. Panda,[†] Tomče Runčevski,*[,‡] Ahmad Husain,[†] Robert E. Dinnebier,[‡] and Panče Naumov*[,†]

[†]New York University Abu Dhabi, P.O. Box 129188, Abu Dhabi, United Arab Emirates
[‡]Max Planck Institute for Solid State Research, Heisenbergstrasse 1, D-70569 Stuttgart, Germany

Supporting Information

ABSTRACT: When heated, single crystals of enantiomerically pure D- and L-pyroglutamic acid (PGA) are capable of recurring self-actuation due to rapid release of latent strain during a structural phase transition, while the racemate is mechanically inactive. Contrary to other thermosalient materials, where the effect is accompanied by crystal explosion due to ejection of debris or splintering, the chiral PGA crystals respond to internal strain with unprecedented robustness and can be actuated repeatedly without deterioration. It is demonstrated that this superelasticity is attained due to the low-dimensional hydrogen-bonding network which effectively accrues internal strain to elicit propulsion solely by elastic deformation without disintegration. One of the two polymorphs (β) associated with the thermosalient phase transition undergoes biaxial *negative* thermal expansion ($\alpha_a = -54.8(8) \times 10^{-6}$ K^{-1}, $\alpha_c = -3.62(8) \times 10^{-6}$ K^{-1}) and exceptionally large uniaxial thermal expansion ($\alpha_b = 303(1) \times 10^{-6}$ K^{-1}). This second example of a thermosalient solid with anomalous expansion indicates that the thermosalient effect can be expected for first-order phase transitions in soft crystals devoid of an extended 3D hydrogen-bonding network that undergo strongly anisotropic thermal expansion around the phase transition.

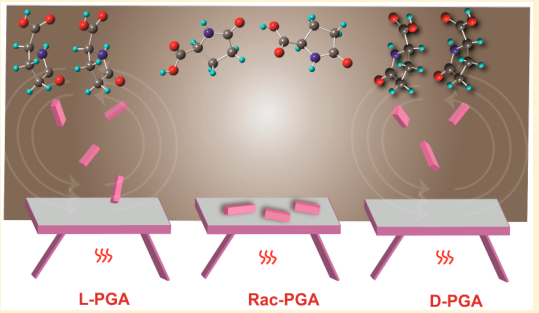

1. INTRODUCTION

The efficiency, durability, and self-healing capability of dynamic biological systems, the outcome of evolution over millennia, continue to inspire materials scientists as structure−functionality principles for design of artificial smart actuators.[1] The principles of operation of biomimetic actuating materials rely on capturing the essence of biogenic actuators in an attempt to emulate their functionality by purposeful modulation of the molecular structure and composition.[2] A multitude of approaches to realization of biogenic actuators have been advanced through the design of single molecules, polymers, and composites where external stimulation by heat, light, humidity, or magnetic/electric field induce structural changes to drive macroscopic motility.[3−6]

Mechanically responsive single crystals are emerging candidates as technomimetic and biomimetic actuating elements that benefit from their ordered three-dimensional structure as medium for efficient harvesting, transfer, and clean conversion of energy.[7−26] However, accomplishing concurrently fast *and* reversible actuation with molecular crystals poses formidable practical challenges; accumulation of internal strain over a long range in their structures is normally detrimental to their macroscopic integrity, which limits their compliance with the most essential requirements for application in actuating modules. The common approach that one resorts to in order to alleviate the detrimental effects of the internal strain is to increase the surface/volume ratio by using slender microcrystals or nanocrystals instead of macrocrystals. However, this does not always provide optimal solution to the problem because of the difficulties with lack of control over the crystal aspect ratio at the nanoscale. A much more restrictive limitation, however, comes from the inherent structure−performance give-and-gain; while very small and/or slender crystals are normally more flexible and resilient to high internal strains, they are also less efficient in performing mechanical work. Aimed at accomplishing reversible mechanical response with preservation of macroscopic crystal integrity, we focused on thermosalient materials (colloquially referred to as "jumping crystals") that incorporate low-dimensional networks of hydrogen bonds, which were recently categorized as type III thermosalient solids.[23,26] These supramolecular constructs conveniently combine hydrogen-bonding networks that absorb the mechanical strain while having a restoring role to preserve crystal integrity. The anisotropy of intermolecular interactions and thermal expansion of the unit cell are critical to acquire and accumulate the strain that elicits a mechanical response.

Herein, a peculiar instance of exceptionally mechanically robust motile single crystals which retain their macroscopic integrity during actuation is reported, and the reasons for this unprecedented resilience are explained. Variable-temperature microscopy revealed that when heated crystals of L- and D-pyroglutamic acid (PGA, Figure 1) are capable of strong, rapid, and recurring self-actuation without disintegration. The same crystals also hop but splinter readily on cooling below ambient temperature. Racemic crystals of PGA are not mechanically active. This first observation of the suppression of the thermosalient effect in a racemic crystal highlights the strongly

Received: October 31, 2014
Published: January 12, 2015

DOI: 10.1021/ja5111927
J. Am. Chem. Soc. 2015, 137, 1895−1902

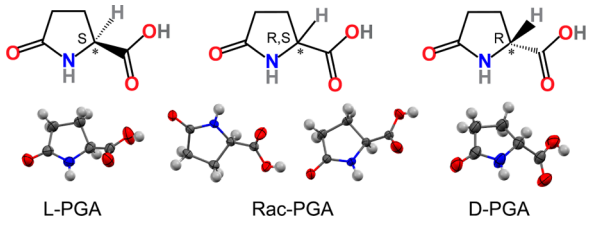

Figure 1. Chemical structures (top) and ORTEP-style plots (bottom; 50% probability) of the molecular structures of L, D, and racemic (Rac) pyroglutamic acid (PGA).

cooperative nature of the underlying structural process, which requires an ordered lattice of molecules with identical configuration to be sustained. The results also provide firm evidence that, contrary to the perception of these effects as highly incongruous and detrimental to the crystal, when induced in elastically complaint structure, the thermosalient effect can become perpetual and occur with sustainable crystal integrity.

2. Results and Discussion. 2.1. Thermosalient effect in PGA crystals. On heating from room temperature (RT), single-crystalline blocks of both L- and D-PGA transition from form α to form β with a spectacular thermosalient effect: The crystals jump fiercely, occasionally hopping off the hot stage (Figures 2a–c and 3c). Movie S1, Supporting Information, shows a lateral view of a crystal of L-PGA performing a vertical jump recorded with a high-speed camera coupled to an optical microscope (the time resolution at which each movie was recorded is available in the movie legends). Movies S2 and S3, Supporting Information, show the motility of crystals of L-PGA and D-PGA, respectively, recorded in a direction perpendicular to the microscope plane (in these videos, the crystals spin and disappear as they propel themselves to travel toward the viewer and go out of the focus). Unlike the few other thermosalient and photosalient materials whose crystals usually splinter or explode during the effect, most of the crystals of PGA were exceedingly robust; in consecutive heating–cooling cycles they could be propelled at least 15 times without any apparent

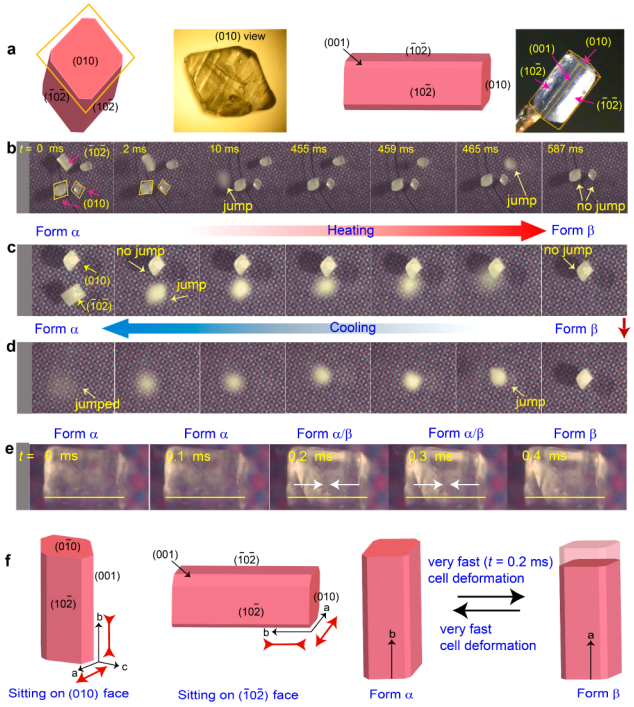

Figure 3. The kinematic behavior of L-PGA crystals is determined by the resting crystal face. (a) Face indices of L-PGA crystals shown on real crystals and on models; (b, c) Kinematic behavior of heated (a; transition $\alpha \rightarrow \beta$) crystals of L-PGA in respect to the crystal face that was in contact with the temperature-controlled surface. Note that the crystals jump when they sit on $(\bar{1}02)/(10\bar{2})$ or $(\bar{1}0\bar{2})/(102)$, but remain static when sitting on (010); (d) On cooling (reverse transition $\alpha \leftarrow \beta$) the crystals sitting on (010) also jump, presumably due to relaxation from the sudden spring-like expansion during the forward transition; (e) Rapid change of the crystal shape during the phase transition $\alpha \rightarrow \beta$. (f) Schematic explanation of the crystal deformation that triggers the thermosalient effect. Crystals sitting on (010) face remain immotile due to the uniform positive thermal expansion (PTE) along the a and c axes. When crystals sit on $(\bar{1}02)/(10\bar{2})$ or $(\bar{1}0\bar{2})/(102)$, they undergo nonuniform PTE along a and b axes whereby they spring off.

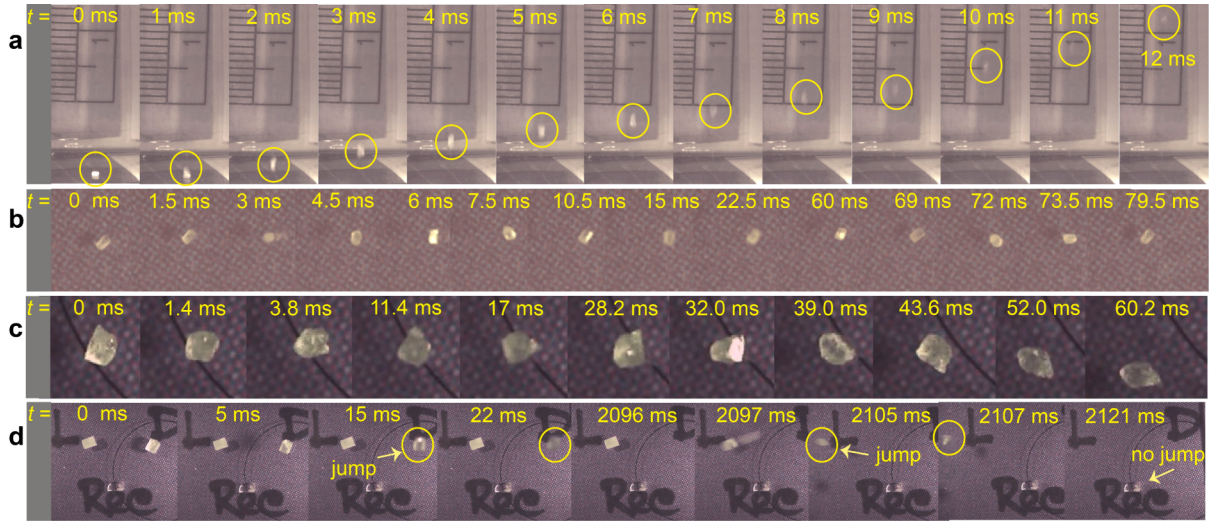

Figure 2. Optical microscopic snapshots extracted from high-speed video recordings of the thermosalient effect in crystals of PGA. (a) Vertical jumps of L-PGA crystals (the distance between the small marks on the ruler scale is 1 mm); (b, c) Motility of L-PGA (b) and D-PGA (c) crystals recorded normal to the plane of the heated microscope stage; (d) Comparison of the motility of L-PGA (L), D-PGA (D) and a racemic crystal (Rac). Note that while both chiral crystals are motile, the racemic crystal remains still.

DOI: 10.1021/ja5111927
J. Am. Chem. Soc. 2015, 137, 1895–1902

disintegration or loss of translucency. Temperature-controlled microscopy (see below) revealed that the chiral PGA crystals are motile not only on heating to high temperature (HT; Movies S4 and S5, Supporting Information) but also on cooling to low temperature (LT; Movies S6 and S7, Supporting Information) due to the transition $\alpha' \leftarrow \alpha$ (Figure 3d). However, unlike the motion at HT, at LT the thermosalient effect was much weaker and irreversible; the cooled crystals hopped, but they turned opaque and rapidly disintegrated.

Heated L/D-PGA crystals always jumped when sitting with their $(\bar{1}02)/(10\bar{2})$, $(\bar{1}0\bar{2})/(102)$, or (001) face on the hot surface (Figure 3a and 3b; Movies S8 and S9, Supporting Information). Interestingly, no motion was observed during the $\alpha \rightarrow \beta$ transition when the crystals sat with their (010) face (Figure 3c; for L-PGA as example, see Movie S10, Supporting Information). However, the crystals jumped during the reverse transition, $\alpha \leftarrow \beta$ (Figure 3d; Movie S11, Supporting Information). Inspection of the high-speed recordings of the thermosalient effect showed that the crystal locomotion occurred as hopping, spinning, rolling, or sliding. In most cases, the crystals hopped fiercely off the stage in the first cycle. In subsequent cycles the mechanical effect was alleviated; however, the hopping continued and the integrity of the crystals remained intact. Heated crystals of D-PGA hopped off the stage around 340 K and rotated several times before landing, without any changes in surface morphology. Crystals of L-PGA were particularly robust; within a set of 30 crystals of L- and D-PGA each examined, cracks on the surface were observed in only a few cases. Figure S2, Supporting Information, shows SEM images of the crystals before and after heating to 365 K. Detailed inspection by optical microscopy, SEM, and AFM of the surface of L-PGA crystals that were taken over the HT thermosalient transition did not show any significant changes in the surface morphology (Figures S16 and S17, Supporting Information). This result indicated that contrary to photochemical reactions such as photodimerizations, where usually a significant mass transfer occurs on the surface of the crystal which results in increased surface roughness, the TS transition in PGA is accompanied by a very small structural rearrangement.

The phase transition $\alpha \rightarrow \beta$ of the chiral crystals was accompanied by a very fast reconfiguration of crystal shape (Figure 3e and 3f; Movie S12, Supporting Information). Crystals of both enantiomers shrunk along their longest side (parallel to the axis b) during the transition and expanded during the reverse transition. On the basis of the kinematic parameters extracted from the high-speed recordings (time resolution 10^4 s^{-1}) of heated crystals of L- and D-PGA, the transition occurs within 2×10^{-4} s. The crystal is transformed with an average linear speed of the progression of the phase front (the habit plane) of 2.8 m s^{-1} (Figure S3, Supporting Information). This result is in line with our previous observations of exorbitantly high speeds related to progression of the habit plane in thermosalient relative to nonthermosalient transitions.[22] By very simple calculation (Figure S1, Supporting Information), the initial average velocity (v_1) of the crystal of approximate size $0.83 \times 0.61 \times 0.47$ mm was estimated to be 0.427 m s^{-1}. The energy generated by the thermosalient effect that lifts the crystal to a height of 19.43 mm was $E \approx 6.51988 \times 10^{-7}$ J, and the power was $P \approx 1.0866 \times 10^{-7}$ J s^{-1}.

In stark contrast to the chiral crystals, the racemic crystals of PGA (Rac-PGA) did not exhibit any mechanical motion and remained still on heating (Figure 2d; Movie S13, Supporting Information) as well as on cooling (Movie S14, Supporting Information; the composition of the racemic crystals was confirmed with circular dichroism spectroscopy; see Figure S4, Supporting Information). Movie S15, Supporting Information, shows the response from two crystals of each of L-PGA, D-PGA, and Rac-PGA of comparable size to avoid size effects on the latent period required for stress accrual (time resolution 10^3 s^{-1}). The crystals of D-PGA hopped first, followed by the crystals of L-PGA. The time lapse between the jump of the second crystal of D-PGA and the jump of the first crystal of L-PGA was 1210 ms, which is a significant delay on the time scale on which these events occur. This hiatus points out to control of the mechanical response by fine details of the crystal structure such as chirality, although this hypothesis requires further verification.

2.2. Thermal Profile of the Thermosalient Effect. The phase transitions of L-PGA were studied by West et al.[27,28] To correlate the mechanical effects with the structure, we reinvestigated in detail the phase transitions of both stereoisomers. Both transitions $\alpha \rightarrow \beta$ and $\alpha' \leftarrow \alpha$ are reversible and display a sawtooth-like profile in the DSC traces characteristic for a process which occurs in bursts similar to martensitic transitions (Figure 4a–d).[23,25,27−30]

In the first thermal cycle, the endothermic process $\alpha \rightarrow \beta$ occurred at 337–338 K (Figure 4d, Table 1). In subsequent cycles the transition temperature decreased to 335–336 K, presumably in effect to structure stabilization, while the crystals continued to hop without disintegration. On cooling to LT, the transparent colorless crystals of both L-PGA and D-PGA also hopped but lost their translucency irrecoverably with visible changes in their surface morphology (Figure 6a and 6b). The related LT transitions ($\alpha' \leftarrow \alpha$) were detected at 131.8–138.6 and 134.8–136.4 K, respectively (Table 1). Contrary to the chiral crystals, the crystals of Rac-PGA remained still on heating as well as on cooling (Figures 5c and 6c). Inspection of the DSC profile of the racemate showed that the lack of mechanical effect is due to the absence of a phase transition between 103 K and the melting point at ~456 K (Figure 4g and 4h).

2.3. Structure Elucidation of the Unknown Phases. While the structures of forms α and α' of L-PGA are known,[27] those of forms α and α' of D-PGA and of forms β of both L-PGA and D-PGA were not determined prior to this study. To establish the complete mechanism of the two thermosalient phase transitions, we determined the structures of forms α and α' L-PGA and D-PGA at various temperatures and also determined for the first time the structure of the β forms of both isomers (for crystallographic details, see Tables S1–S12, Supporting Information). Crystals of form β of both isomers were obtained in situ by heating single crystals of form α with hot nitrogen (80 °C). X-ray diffraction analysis of forms α and α' confirmed the reported unit cells.[27,31]

The fortuitous occurrence of two phase transitions and both strong (HT) and weak (LT) thermosalient effects in a single system provides insight into the driving force of crystal motility. Figure 7 shows the crystallographic relationships between the structures of the three forms, and Table 1 contains the relevant crystallographic details (see also Figures S5–S10 and Tables S1–S3 and S12, Supporting Information). There are three independent PGA molecules in the asymmetric unit of forms α and α' of L/D-PGA but only one in form β. During the LT phase transition ($\alpha' \leftarrow \alpha$), the unit cells of both L- and D-PGA contract along the a axis (−9.28% for L-PGA and −8.99% for D-PGA) and expand along the b axis (+6.53% for L-PGA and

DOI: 10.1021/ja5111927
J. Am. Chem. Soc. 2015, 137, 1895–1902

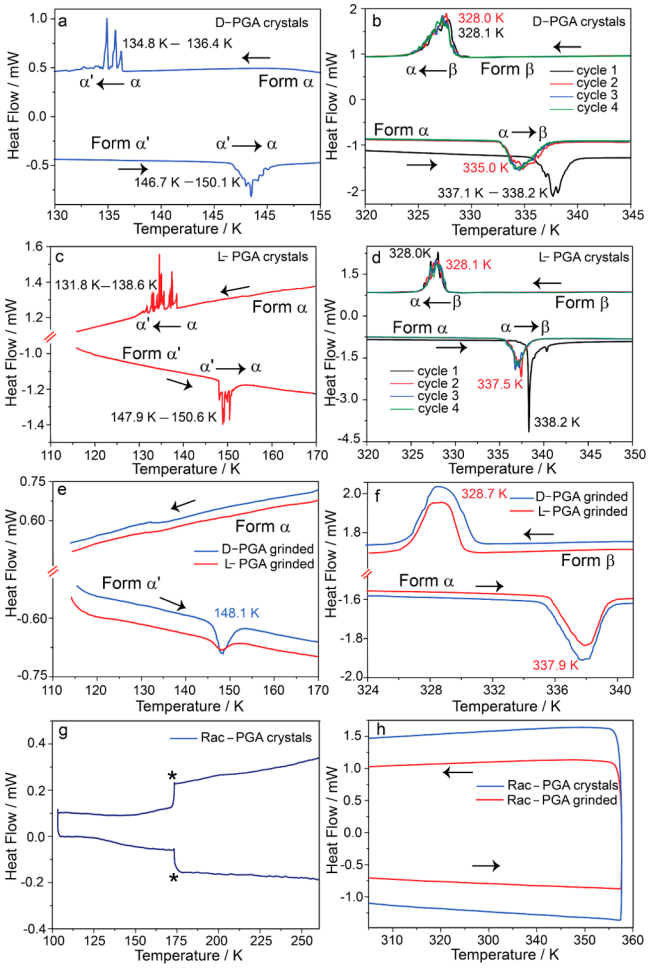

Figure 4. Thermal profile of the phase transitions in D, L, and racemic (Rac) crystals of PGA monitored by DSC. HT and LT phase transitions in as-obtained crystals of D-PGA (a, b), L-PGA (c, d), grinded D/L-PGA (e, f), and racemic PGA (Rac-PGA; g, h). Note that the Rac-PGA crystals do not undergo a phase transition between 100 and 360 K (the steep changes in the heat flow in panel g marked with asterisks are artifacts of the changes in the cooling rate).

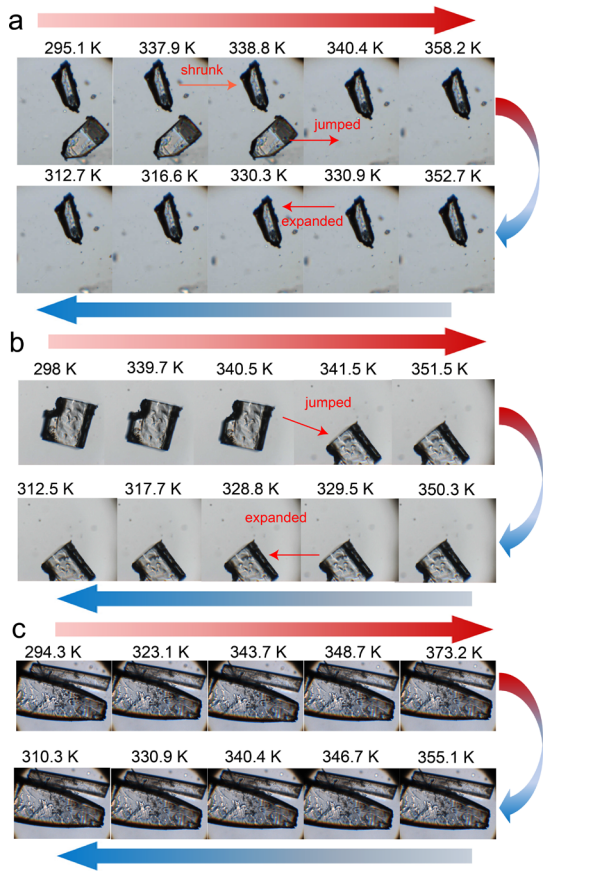

Figure 5. High-temperature thermosalient effect of L-PGA (a), D-PGA (b), and racemic PGA (c) observed with variable-temperature optical microscopy. Red and blue arrows indicate heating and cooling, respectively.

+6.62% for D-PGA). The change is negligible along the *c* axes of both L- and D-PGA, giving ∼3% overall volume contraction. During the HT transition $\alpha \rightarrow \beta$, the *a* and *b* axes of L/D-PGA are exchanged. The *a* axis expands (+1.58% for L-PGA and 1.66% for D-PGA), the *c* axis expands slightly (0.55% for L-PGA and 0.57% for D-PGA), whereas the *b* axis, which corresponds to 1/3 of the original axis, shrinks (−1.57% for L-PGA and −1.35% for D-PGA). The unit cell (per formula unit) during the $\alpha \rightarrow \beta$ transition expands only ∼+0.53% for L-PGA and ∼+0.86% for D-PGA, in line with the earlier conclusions that the TS effect does not necessarily require large volume change.[23] The similarity index calculated with XPac[32,33] indicated greater similarity between forms α and β (100% and 75% for L- and D-PGA, respectively) relative to forms α and

Table 1. Phase Transition Temperatures and Unit Cell Distortions during the Thermosalient Transitions in L- and D-PGA

isomer, transition	*T*/K (DSC)	form	*a* axis/Å	*b* axis/Å	*c* axis/Å	cell volume, *V* / Å^3
L-PGA	131.8−138.6	α^a	9.024(5)	13.453(8)	14.672(8)	1781.1(18)
$\alpha \rightarrow \alpha'$	147.9−150.6	α'^b	8.1865(3)	14.3317(5)	14.6585(5)	1719.83(10)
$\alpha' \rightarrow \alpha$		$\Delta/\%^e$	−9.28	+6.53	−0.0009	−3.4
L-PGA	338.2−340.4	α^a	9.024(5)	13.453(8)	14.672(8)	1781.1(18)
$\alpha \rightarrow \beta$	328.7−326.9	β^c	4.4135(7)	9.1662(14)	14.753(2)	596.85(16)
$\beta \rightarrow \alpha$		$\Delta/\%^e$	+1.58	−1.57	+0.55	+0.53
D-PGA	134.8−136.4	α^a	9.0121(12)	13.4568(18)	14.6634(18)	1778.3(4)
$\alpha \rightarrow \alpha'$	146.7−150.1	α'^b	8.2013(8)	14.3479(14)	14.6577(13)	1724.8(3)
$\alpha' \rightarrow \alpha$		$\Delta/\%^e$	−8.99	+6.62	−0.0004	−3.0
D-PGA	336.3−338.1	α^a	9.0121(12)	13.4568(18)	14.6634(18)	1778.3(4)
$\alpha \rightarrow \beta$	328.7−325.1	β^d	4.4250(10)	9.162(2)	14.747(3)	597.9(2)
$\beta \rightarrow \alpha$		$\Delta/\%^e$	+1.66	−1.35	+0.57	+0.86

[a]Unit cell parameters determined at 300 K. [b]At 130 K. [c]At 353 K. [d]At 360 K. [e]The esd's were not considered in the calculation.

DOI: 10.1021/ja5111927
J. Am. Chem. Soc. 2015, 137, 1895−1902

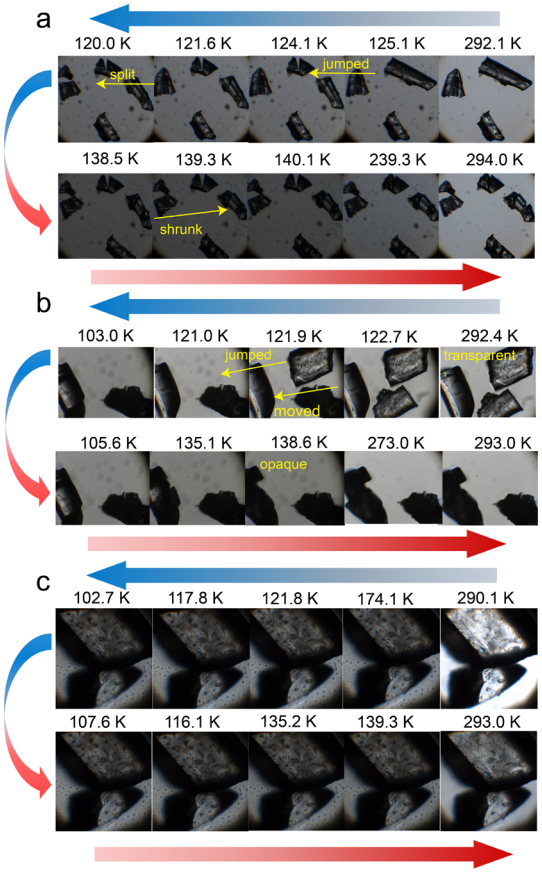

Figure 6. Low-temperature thermosalient effect of L-PGA (a), D-PGA (b), and racemic PGA (c) observed with variable-temperature optical microscopy. Red and blue arrows indicate heating and cooling, respectively.

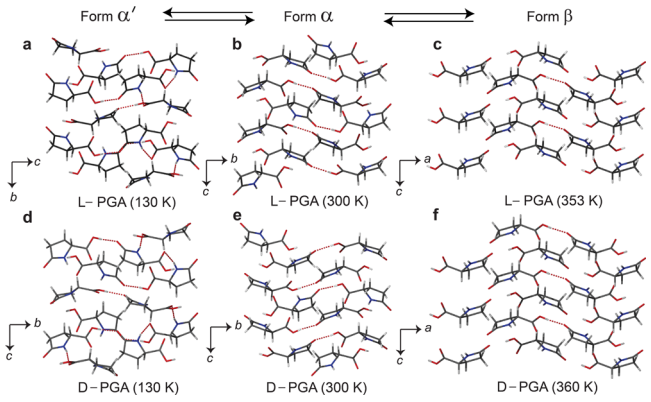

Figure 7. Crystal packing of the three polymorphs of L-PGA (a–c) and D-PGA (d–f). Structures of forms α' and α are presented as viewed down the a axes, while the β forms are viewed down the b axes (equivalent to a axis of forms α' and α). The unit cell content of form β was tripled for comparison with forms α' and α.

α' (58% for both L- and D-PGA), indicating that the preservation of macroscopic integrity of the crystal during the HT thermosalient transition is rooted in greater overall packing similarity between forms α and β (Figures S6, S7, and S18, Supporting Information).

During the LT thermosalient transition ($\alpha' \leftarrow \alpha$), the hydrogen-bonding network (Figure 7) is conserved and only changes in intermolecular distances were observed. This small change is consistent with those in other thermosalient solids, where diffusionless "military"[34] transitions with very small or no changes in intermolecular disposition have been invariably observed. Thus, the thermosalient effect at LT is accredited to sharp and anisotropic change in lattice parameters. The accumulation of internal strain in the crystal structures would normally have a detrimental effect to the macroscopic crystal integrity. Adjustments in hydrogen-bonding network that accompany switching of the structure to form β effectively accommodates the structure perturbation to dissipate that strain (Figure 8, see also Figure S10, Supporting Information).

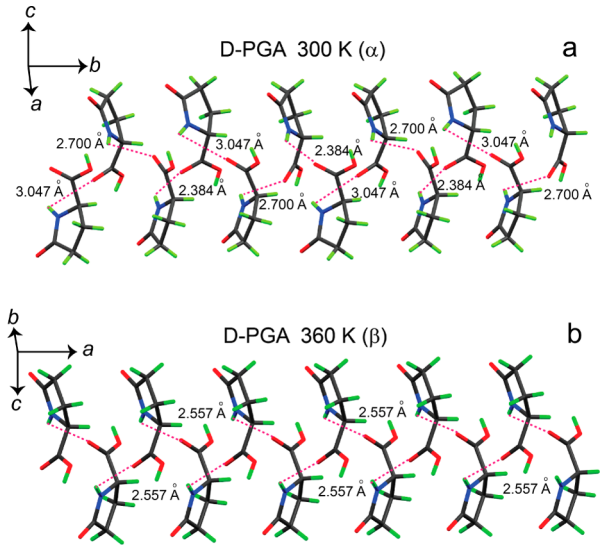

Figure 8. Hydrogen bonding in the crystals of forms α (a) and β (b) D-PGA.

Preliminary information on the thermal response of the unit cell was obtained from single-crystal X-ray diffraction data (Figures S11–S15, Supporting Information). A higher density of data at a smaller temperature increment required for calculation of the thermal expansion was obtained for forms α and β L-PGA by fitting the variable-temperature high-resolution X-ray powder diffraction patterns with the linear formula $p = p_0 \exp[\alpha_p(T - T_0)]$ (Figure 9). Because both forms have orthorhombic symmetry, the principle thermal expansion coefficients coincide with the coefficients calculated along the crystallographic axes.[35] Form α shows stronger than normal thermal expansion along the a and c axes, with $\alpha_a = 43.4(7) \times 10^{-6}$ K^{-1} and $\alpha_c = 23.7(4) \times 10^{-6}$ K^{-1}, and considerably strong TE along the b axis, $\alpha_b = 105.5(5) \times 10^{-6}$ K^{-1} (typical values for molecular solids are $0–20 \times 10^{-6}$ K^{-1} [36]). The respective volumetric coefficient is $\alpha_V = 171.7(8) \times 10^{-6}$ K^{-1}. Form β, on the other hand, shows a peculiar thermal expansion where *two* axes undergo *negative* thermal expansion (contraction) with $\alpha_a = -54.8(8) \times 10^{-6}$ K^{-1} and $\alpha_c = -3.62(8) \times 10^{-6}$ K^{-1} and the b axis undergoes exceptionally strong uniaxial thermal expansion with $\alpha_b = 303(1) \times 10^{-6}$ K^{-1}. The uniaxial expansion and biaxial contraction gives a high positive volumetric thermal coefficient of $245(2) \times 10^{-6}$ K^{-1}. Double negative axial thermal expansion is an extremely rarely observed behavior.[37] Some of us recently reported a very strong thermal expansion in a thermosalient palladium organometallic material,[22] which indicates a possible relationship between the mechanical effect

DOI: 10.1021/ja5111927
J. Am. Chem. Soc. 2015, 137, 1895–1902

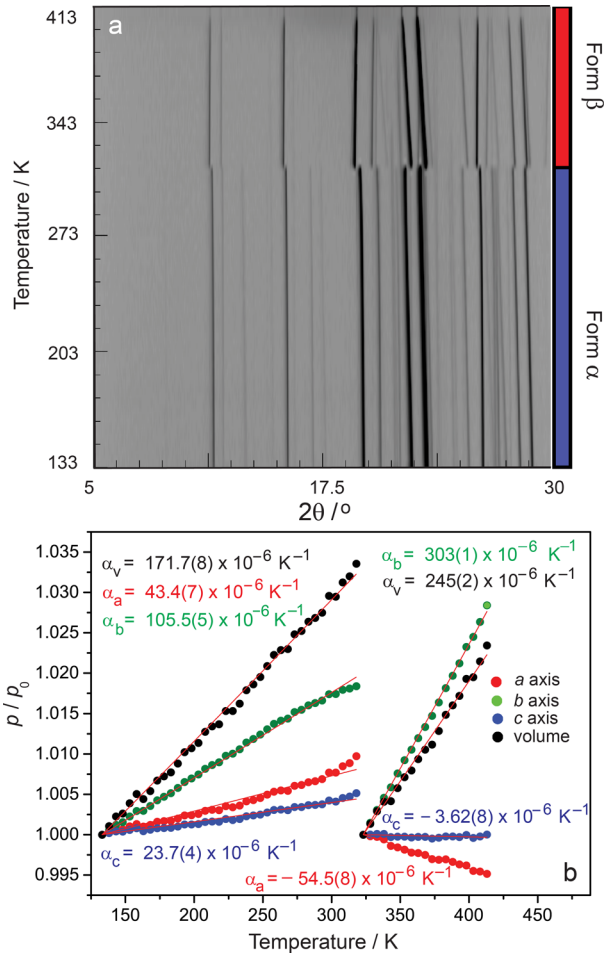

Figure 9. (a) 2D Projection of the scattered X-ray intensity of L-PGA as a function of temperature and diffraction angle. (b) Temperature change of unit cell parameters fitted with a linear equation, $p = p_0 \exp[\alpha_p(T - T_0)]$.

and the strong, anisotropic thermal expansion in thermosalient solids.

3. CONCLUSIONS

The thermosalient effect is rarely observed and almost never reported phenomenon. What once was a mere curiosity in crystals popping when heated, now starts to reveal rich and exciting crystal chemistry and new, previously unexplored properties and unrecognized potential of molecular crystals. As common properties, the few recently studied examples of the thermosalient effect are consistent with an isosymmetric (preserved space group), diffusionless, first-order phase transition which resembles the transitions observed with inorganic martensites. The volume change accompanying the transition is small but invariably anisotropic.[23] The spatial progression of the phase front is much faster than those in other, nonthermosalient transitions. Nanoindentation assessment showed that these structures are unusually soft.[38] We believe that the softness holds the key for their susceptibility to high internal strains with delayed phase change, up to the point where the transition is triggered (for example, by a defect site or at the corners) and advances very rapidly throughout the crystal.

Here, we investigated the structure−kinematic relations in the only known chiral thermosalient material, PGA. This organic martensite is special for several reasons; crystals of both chiral forms undergo thermosalient effects on cooling as well as on heating, and the effect occurs with unprecedented robustness where the crystal integrity is completely retained during the HT phase transition even after multiple thermal cycles, while the LT transition is accompanied by immediate disintegration. An unexpected but ostensibly very important observation from a mechanistic viewpoint is the observation that although both chiral forms undergo phase transition, the racemic crystal is completely inert. The absence of phase transition translates in a lack of mechanical reconfiguration of the racemic crystals. This result points to the importance of the regularity in the molecular configuration which is critical for cooperative action for macroscopic actuation. The small structural changes that would be expected to accompany the phase transition of the racemate are evident from the overlapped packing models of the structures of L-PGA and the racemic crystals (Figure S18, Supporting Information).

Similar to the only other thermosalient solid that was investigated in detail (class I thermosalient solid),[22] with PGA (class III thermosalient solid)[23] we observed anomalous thermal expansion, which adds to the characteristics that are common for materials that exhibit the thermosalient effect. Form α shows larger than usual thermal expansion along the a and c axes and considerably large thermal expansion along the b axis. In form β, on the other hand, two axes (a and c) undergo negative thermal expansion, while the b axis undergoes exceptionally large uniaxial thermal expansion. The similarities in the thermal behavior of PGA, an organic molecule, and a palladium complex reported previously[22] point out a strongly anisotropic distortion of the structure before it undergoes thermosalient transition. These results indicate that in a quest for other thermosalient structures one should seek a soft material, devoid of tridimensional hydrogen bonding, which exhibits anomalous thermal expansion (strong positive and/or negative expansion) and undergoes a phase transition on heating or cooling. The recent advances in the application of nanoindentation analysis have provided new insights into the mechanical properties of molecular crystals[38−43] and promise a new venue for discovery of thermosalient solids.

4. EXPERIMENTAL METHODS

4.1. Materials. Crystalline L-PGA (CAS no. 98-79-3) and D-PGA (CAS no. 4042-36-8) were obtained from Aldrich and used as received. Racemic PGA (CAS no. 149-87-1) was obtained from Aldrich and recrystallized by slow evaporation from methanol.

4.2. Thermal Analysis. Differential scanning calorimetry was carried out on TA DSC-Q2000 instrument. Typically, PGA samples (crystals or powder) were taken on a Tzero aluminum pan and heated from RT (300 K) to the selected temperature at a rate of 10 K min^{-1} for HT (300−370 K) runs. For the low-temperature study, the cooling rate was 5 K min^{-1} in the 298−173 K range and 2 K min^{-1} in the 173−100 K range and in dynamic atmosphere of helium (flow rate 50 mL min^{-1}).

4.3. X-ray Diffraction (XRD). Single-crystal XRD data was collected on a Bruker APEX DUO diffractometer with monochromated Mo Kα radiation (λ = 0.71069 Å) and CCD as the area detector.[44] All crystallographic calculations were performed using the crystallographic software APEX 2.[44] The data were reduced with SADABS,[45] and the structures were determined by the intrinsic method.[46,47] The non-hydrogen atoms were refined anisotropically.[48] Unit cell parameters from very good crystals of L-PGA and D-PGA were determined by 10 s exposure at 10 K intervals starting from 300 to 140 K. The parameters were refined using similar number of reflections (about 380 reflections with a tolerance limit of ~0.45). In

DOI: 10.1021/ja5111927
J. Am. Chem. Soc. 2015, 137, 1895−1902

most cases below 140 K crystals jumped due to the LT phase transition and reliable lattice parameters could not be obtained below the phase transition temperature. An excessive amount of glue was used to retain a crystal of D-PGA in place, and data were collected down to 100 K. The number of reflections decreased from 568 at 140 K to 232 at 130 K, and only 82 reflections could be indexed with a maximum tolerance out of 232 reflections without a reliable unit cell. High-resolution X-ray powder diffraction (XRPD) data were collected on a laboratory powder diffractometer Stoe Stadi-P with Cu $K\alpha_1$ radiation from primary Ge(111)-Johannson-type monochromator and Dectris-MYTHEN 1K strip PSD with an opening angle of 12° in 2θ, in Debye–Scherrer geometry.

4.4. Microscopy. The thermomicroscopic behavior of PGA crystals was analyzed with a hot-stage microscope (Linkam) consisting of a temperature-controlled stage THMS600-PS mounted on Q-imaging (Q32643) microscope. Samples were heated or cooled to specific temperature from RT (300 K) at a constant heating rate of 5 K min^{-1}. Atomic force microscopy (AFM) at RT was preformed on an Agilent 5500 system in ac ("tapping") mode. Cantilever tips with a nominal tip radius of <7 nm were used with a resonant frequency of 287 kHz. Scan arrays were 30 μm × 30 or 50 μm × 50 μm, and the scan speed was ~0.5 lines/s. In the case of rough surfaces, the scan area was reduced appropriately. Feedback control parameters were optimized for each scan. All images were processed and analyzed using the Gwyddion software. The scanning electron microscopy (SEM) experiments were carried out with a QUANTA FEG 450 electron microscope with a primary electron energy of 2–5 kV. The crystals were affixed to a silicon wafer with oil or adhesive, and images were taken before and after heating the crystals to 365 K.

To investigate the effects of the transition on the surface morphology, two batches of L-PGA crystals were hand picked. The surface of the first batch was analyzed (RT) by using AFM and SEM. The crystals of the second batch were taken over the thermosalient transition by heating to 253 K in a closed container, collected, and analyzed (RT) by AFM and SEM. No significant difference in the surface mophology could be detected between the two batches.

4.5. Kinematic Analysis. High-speed recordings were obtained by a HotShot 1280 CC camera (NAC) mounted on a Stereozoom SMZ745T trinocular stereoscope (Nikon). To quantify the energy and efficiency of the work performed by the crystals in the course of the thermosalient effect, a simple procedure was used to calculate the basic kinematic parameters. Figure S1, Supporting Information, shows a schematic representation of the trajectory of a crystal performing a vertical jump. The crystal jumps off the surface with initial maximum velocity (v_1), and its velocity gradually slows down to zero as it reaches the maximum height (h), before it starts to descend. The energy (E) needed to lift the crystal of mass m to height h against gravity equals the work done by the crystal to lift itself to the same height. This energy can be calculated as E = force (F) × displacement (h) = mg × h, where g is the acceleration due to gravity. It should be noted that a more rigorous treatment should include the effect of drag from air, which could be substantial at the scale of the crystal dimensions.

■ ASSOCIATED CONTENT

Supporting Information

Movies of crystal motions recorded with a high-speed camera, microscopic images, thermal analysis results, crystal metrics, crystallographic data, Rietveld refinements. This material is available free of charge via the Internet at http://pubs.acs.org.

■ AUTHOR INFORMATION

Corresponding Authors

*t.runcevski@fkf.mpg.de

*pance.naumov@nyu.edu

Author Contributions

The manuscript was written through contributions of all authors. All authors have given approval to the final version of the manuscript.

Notes

The authors declare no competing financial interest.

■ ACKNOWLEDGMENTS

We thank New York University Abu Dhabi for financial support of this work. Dedicated to Professor Martin Jansen on the occasion of his 70th birthday.

■ REFERENCES

(1) Burgert, I.; Fratzl, P. *Philos. Trans. R. Soc. A* **2009**, *367*, 1541–1557.

(2) Sanchez, C.; Arribart, H.; Guille, M. M. G. *Nat. Mater.* **2005**, *4*, 277–288.

(3) He, X.; Aizenberg, M.; Kuksenok, O.; Zarzar, L. D.; Shastri, A.; Balazs, A. C.; Aizenberg, J. *Nature* **2012**, *487*, 214–218.

(4) Iamsaard, S.; Aßhoff, S. J.; Matt, B.; Kudernac, T.; Cornelissen, J. J. L. M.; Fletcher, S. P.; Katsonis, N. *Nat. Chem.* **2014**, *6*, 229–235.

(5) Xia, F.; Jiang, L. *Adv. Mater.* **2008**, *20*, 2842–2858.

(6) Shepherd, H. J.; Gural'skiy, I. A.; Quintero, C. M.; Tricard, S.; Salmon, L.; Molnár, G.; Bousseksou, A. *Nature Commun.* **2013**, *4*, 2607.

(7) Kobatake, S.; Takami, S.; Muto, H.; Ishikawa, T.; Irie, M. *Nature* **2007**, *446*, 778–781.

(8) Terao, F.; Morimoto, M.; Irie, M. *Angew. Chem., Int. Ed.* **2012**, *51*, 901–904.

(9) Morimoto, M.; Irie, M. A. *J. Am. Chem. Soc.* **2010**, *132*, 14172–14178.

(10) Kitagawa, D.; Nishi, H.; Kobatake, S. *Angew. Chem., Int. Ed.* **2013**, *52*, 9320–9322.

(11) Kim, T.; Al-Muhanna, M. K.; Al-Suwaidan, S. D.; Al-Kaysi, R. O.; Bardeen, C. J. *Angew. Chem., Int. Ed.* **2013**, *52*, 6889–6893.

(12) Kim, T.; Zhu, L.; Al-Kaysi, R. O.; Bardeen, C. J. *ChemPhysChem* **2014**, *15*, 400–414.

(13) Zhu, L.; Al-Kaysi, R. O.; Bardeen, C. J. *J. Am. Chem. Soc.* **2011**, *133*, 12569–12575.

(14) Yakobson, B. I.; Boldyreva, E. V.; Sidelnikov, A. A. *Proc. Sib. Dept. Acad. Sci. USSR* **1989**, *51*, 6–10.

(15) Boldyreva, E. V.; Sidelnikov, A. A.; Rukosuev, N. I.; Chupakhin, A. P.; Lyakhov, N. Z. Patent SU 1368654, 1985.

(16) Ghosh, S.; Reddy, M. C. *Angew. Chem., Int. Ed.* **2012**, *51*, 10319–10323.

(17) Abakumov, G. A.; Nevodchikov, V. I. *Dokl. Akad. Nauk SSSR* **1982**, *266*, 1407–1410.

(18) Lange, C. W.; Földeaki, M.; Nevodchikov, V. I.; Cherkasov, V. K.; Abakumov, G. A.; Pierpont, C. G. *J. Am. Chem. Soc.* **1992**, *114*, 4220–4222.

(19) Pierpont, C. G. *Proc. Indian Acad. Sci., Chem. Sci.* **2002**, *114*, 247–254.

(20) Koshima, H.; Ojima, N.; Uchimoto, H. *J. Am. Chem. Soc.* **2009**, *131*, 6890–6891.

(21) Koshima, H.; Takechi, K.; Uchimoto, H.; Shiro, M.; Hashizume, D. *Chem. Commun.* **2011**, *47*, 11423–11425.

(22) Panda, M. K.; Runčevski, T.; Sahoo, S. C.; Belik, A. A.; Nath, N. K.; Dinnebier, R. E.; Naumov, P. *Nat. Commun.* **2014**, *5*, 4811.

(23) Sahoo, S. C.; Panda, M. K.; Nath, N. K.; Naumov, P. *J. Am. Chem. Soc.* **2013**, *135*, 12241–12251.

(24) Naumov, P.; Sahoo, S. C.; Zakharov, B.; Boldyreva, E. *Angew. Chem., Int. Ed.* **2013**, *52*, 9990–9995.

(25) Skoko, Ž.; Zamir, S.; Naumov, P.; Bernstein, J. *J. Am. Chem. Soc.* **2010**, *132*, 14191–14202.

(26) Nath, N. K.; Panda, M. K.; Sahoo, S. C.; Naumov, P. *CrystEngComm* **2014**, *16*, 1850–1858.

(27) Wu, H.; Reeves-McLaren, N.; Pokorny, J.; Yarwood, J.; West, A. R. *Cryst. Growth Des.* **2010**, *10*, 3141–3148.

(28) Wu, H.; West, A. R. *Cryst. Growth Des.* **2011**, *11*, 3366–3374.

(29) Kaneko, F.; Yano, J.; Tsujiuchi, H.; Tashiro, K. *J. Phys. Chem., B* **1998**, *102*, 327–330.

DOI: 10.1021/ja5111927
J. Am. Chem. Soc. 2015, 137, 1895–1902

(30) Crawford, M.-J.; Evers, J.; Göbel, M.; Klapötke, T. M.; Mayer, P.; Oehlinger, G.; Welch, J. M. *Propellants Explos. Pyrotech.* **2007**, *32*, 478−495.
(31) van Zoeren, E.; Oonk, H. A. J.; Kroon, J. *Acta Crystallogr., Sect. B* **1978**, *34*, 1898−1900.
(32) Gelbrich, T.; Hursthouse, M. B. *CrystEngComm* **2005**, *7*, 324−336.
(33) Gelbrich, T.; Hursthouse, M. B. *CrystEngComm* **2006**, *8*, 448−460.
(34) Krumhansl, J. A.; Yamada, Y. *Mater. Sci. Eng., A* **1990**, *127*, 167−181.
(35) Cliffe, M.; Goodwin, A. *J. Appl. Crystallogr.* **2012**, *45*, 1321−1329.
(36) Krishnan, R. S.; Srinivasan, R.; Devanarayanan, S. *Thermal Expansion of Crystals*; Pergamon: New York, 1979.
(37) Das, D.; Jacobs, T.; Barbour, L. J. *Nat. Mater.* **2010**, *9*, 36−39.
(38) Sahoo, S. C.; Sinha, S. B.; Kiran, M. S. R. N.; Ramamurty, U.; Dericioglu, A. F.; Reddy, M. C.; Naumov, P. *J. Am. Chem. Soc.* **2013**, *135*, 13843−13850.
(39) Karunatilaka, C.; Bučar, D.-K.; Ditzler, L. R.; Friščić, T.; Swenson, D. C.; MacGillivray, L. R.; V. Tivanski, A. V. *Angew. Chem., Int. Ed.* **2011**, *50*, 8642−8646.
(40) Reddy, C. M.; Padmanabhan, K. A.; Desiraju, G. R. *Cryst. Growth. Des.* **2006**, *6*, 2720−2731.
(41) Varughese, S.; Kiran, M. S. R. N.; Ramamurty, U.; Desiraju, G. R. *Angew. Chem., Int. Ed.* **2013**, *52*, 2701−2712.
(42) Chen, C.-T.; Ghosh, S.; Reddy, C. M.; Buehler, M. J. *Phys. Chem. Chem. Phys.* **2014**, *16*, 13165−13171.
(43) Reddy, C. M.; Gundakaram, R. C.; Basavoju, S.; Kirchner, M. T.; Padmanabhan, K. A.; Desiraju, G. R. *Chem. Commun.* **2005**, 3945−3947.
(44) *APEX DUO, version 2.1-4, and SAINT, version 7.34A*; Bruker AXS Inc.: Madison, WI, 2012.
(45) Sheldrick, G. M. *SADABS*; University of Göttingen, Göttingen, Germany, 1996.
(46) Sheldrick, G. M. *Acta Crystallogr., Sect. A* **2008**, *64*, 112−122.
(47) Sheldrick, G. M. *SHELXS-97*; University of Göttingen: Göttingen, Germany, 2008.
(48) Sheldrick, G. M. *SHELXL-97*; University of Göttingen: Göttingen, Germany, 2008.

DOI: 10.1021/ja5111927
J. Am. Chem. Soc. 2015, 137, 1895−1902